Liquid-Vapor Phase Transition and Bubble Formation in Micro Structures*

Liwei LIN, † Kent S. UDELL † and Albert P. PISANO †

Abstract

The formation of vapor bubbles on a micro heater inside micromachined channels is studied. The micro channels consist of silicon nitride side walls fabricated on silicon substrates and "capped" by transparent silicon nitride films. These channels have trapezoidal cross sections of 30 and 60 μm width and 7.5 μm depth. Both constant cross sectional area and variable cross sectional channels (diverging shaspes) have been fabricated and tested with both DC and AC inputs to the micro heaters. The micro heater has a typical dimension of $0.3x2x50\ \mu m^3$ and are made of heavily phosphorus doped polysilicon. The micro bubble formation process is observed under a microscope, recorded on video tape and photographed. Maximum surface temperatures on the micro heaters are calculated by a lumped one-dimensional model. The nucleation temperature is observed to be close to the critical point of the three liquids tested (water, methanol and Fluorinert 43). Bubble movement due to variable channel dimensions and Marangoni effects are observed.

KEYWORDS: *Point contact, Thermoelectric power, Tunneling effect*

Nomenclature

c_p	=	specific heat of polysilicon
J	=	current density
L	=	length of the heater
k_n	=	thermal conductivity of silicon nitride
k_o	=	thermal conductivity of silicon dioxide
k_{no}	=	thermal conductivity of the thermal barrier (silicon dioxide and nitride layers)
k_p	=	thermal conductivity of polysilicon
P_g	=	electrical energy dissipated in the differential element
$\dot{q}_{cond}$	=	heat conduction term in the differential element
$\dot{q}_{conv}$	=	heat convection term in the differential element
$\dot{q}_{rad}$	=	heat radiation term in the differential element
F_s	=	conductive excess flux shape factor
T	=	temperature along the micro heater
$T_{s.s.max}$	=	steady state maximum temperature on the micro heater
$T(x)_{s.s}$	=	steady state temperature along the micro heater
$T(x,t)_{trans}$	=	transient temperature along the micro line heater
T_0	=	ambient temperature
T_r	=	reference temperature in heat equation
t	=	time
t_n	=	thickness of silicon nitride

1 Introduction

Multiphase heat transfer and fluid flow in micro channels have been topics of interest for years in various fields from biology, where blood cell movement in capillaries has been investigated, to petroleum engineering, where oil drop movement through small rock pores is of economic importance. In 1981, Tuckerman [1] used silicon processed micro channels for liquid cooling of VLSI circuits. This approach provided a new methodology for chip cooling and stimulated research in micro heat and mass transfer in silicon processed micro channels. Subsequently, circular micro channels of 360 μm diameters [2] have been made by 3M company, and rectangular micro channels with cross section area of 80 to 7200 μm^2 have been fabricated and tested by Pfahler et al. [3,4]. In addition to the experimental work mentioned above, theoretical work has been presented, including micro-heat exchangers [5], forced convection in micro channels [6], and modeling of micro heat pipes [7].

Recently, advanced IC fabrication tech- nologies have allowed more advanced research in heat and mass transfer on the micro scale; many experimental studies of heat transfer and phase change on the micro scale can now be designed and carried out. In previous work [8], bubble formation on a micro line heater in an open environment was presented. Controllable bubble sizes and Marangoni effects (which affect the micro bubble movements) were demonstrated in that study. Furthermore, a micro bubble powered actuator fabricated by surface micromachining and operated by micro bubbles has been successfully demonstrated [9].

Phase change processes on a heated surface have been under investigation for many years. Cavity theory is cited in most literature for explaining bubble formation for macro machined surfaces. However, the micro heaters used in this paper have micromachined surfaces that are only 1 or 2 μm in width. Current literature relevant to this geometry is not readily available. In previous work [8], the bubble formation temperature was experimentally found to be near the critical point of the liquid. Other researchers also experimentally reported [10,11] and theoretically demonstrated [12] similar results.

Fabrication, modeling and testing of bubble formation on IC fabricated micro line heaters in confined and unconfined micro channels are presented. A heat transfer model is proposed and the theoretical calculations are used to interpret experimental observations. Unlike the bulk micromachined channels mentioned above, transparent, surface micro-machined channels [13,14] have been fabricated with built-in micro line heaters to create micro bubbles. These micro channels are made of low stress, LPCVD (Low Pressure Chemical Vapor Deposition) silicon rich silicon nitride films and have typical cross sections of 30 to 60

* Received: Oct. 15, 1993

† Berkeley Sensor and Actuator Center, Dept.of Mechanical Engineering, University of California (497 Cory Hall University of California, Berkeley, CA 94720)

μm width and 7.5 μm thickness. Both constant cross sectional area and variable cross sectional channels (diverging channels) have been fabricated and tested by both DC and AC inputs to the micro heaters. The heaters are made with LPCVD phosphorus doped polysilicon. These micro channels have a particular useful property - they are optically transparent so that micro bubble formation and micro flow can be observed under optical microscopes. To the best of the authors" knowledge, this is the first presentation of research where the formation of micro bubbles have been observed within the confines of micro channels.

2 Design, Fabrication and Experimental Setup

Figure 1 shows one of the micro channel designs with confined and unconfined portions. It has a total length of 650 μm and width of 60 μm. To facilitate fluid flow into the micro channel, there are 4 fluid inlet/outlet holes of 20x15 μm^2 on both sides and two larger holes of 50x35 μm^2 on the top and bottom portions of the micro channel. The two confined portions have divergent shapes, with the width of the top one increasing from 30 μm to 60 μm, and with the bottom one increasing from 10 μm to 60 μm. Five sets of heating resistors with different dimensions and numbers of micro line heaters are placed along the longitudinal direction of the micro channel. The top two single heaters have the same width of 1 μm and different lengths of 50 and 30 μm respectively. The next confined channel has a set of three heaters with 30 μm length and 3, 2, and 1 μm width from top to bottom. The following downward confined channel portion has a set of heaters of 10 μm in length and 1, 2, and 3 μm in width from top to bottom. The last heater has a dimension of 50x2 μm^2. All heaters have a thickness of 0.36 μm and are connected to two contact pads for power input. The performance of these heaters will be described later.

The micro heaters and micro channels are fabricated by using standard IC processes. Three masks are needed. Figure 2 shows the process sequence. Fabrication begins with <100> N-type prime wafers. Wet oxidation at 110 °C for one hour produces a 0.8 μm thick layer of silicon dioxide layer. The silicon dioxide layer serves as the thermal barrier underneath the micro heater as well as an electronic insulation layer. A LPCVD (Low Pressure Chemical Vapor Deposition) silicon rich silicon nitride layer, 0.35 μm thick, is deposited to serve as the bottom layer of the micro channels. LPCVD *in situ* phosphorus-doped polysilicon deposition is followed to create a 0.5 μm thick layer. A 30 minute, 95 °C anneal is then performed to activate the dopants in the polysilicon. The micro heaters are then defined by mask #1 and plasma dry etched to form the micro heaters and driving pads. The wafers are then twice subjected to three hours of PSG (phosphosilicate glass) deposition to form a 7.5 μm thick PSG layer. This PSG layer is then lithographed to define the channel and the PSG layer is etched by 5:1 buffered HF (hydrofluoric acid). A layer of 1.5 μm thick LPCVD silicon-riched silicon nitride is then deposited to form the top and sides of the channel. The wafers are then plasma etched with mask #3 to produce the fluid inlet and outlet holes and contact pad openings. The PSG left inside the channel for forming the shape of the micro channels is now etched in concentrated HF for 3 minutes. The wafers are finally rinsed in deionized water and dried under an infrared lamp.

Figure 3 shows the SEM photo of a fabricated micro channel with the same design shown in Figure 1. Figure 4 is the SEM view of the divergence portions in Fig. 3. The wet etching process which defines the side walls of the channel gives the cross section of the micro channels a trapezoidal shape instead of a rectangular shape as shown by the SEM shown in Figure 5, where the 30 μm portion of the divergence portion is shown. The top of the channel has a triangular shape with the center about 1.5 μm higher than the edge. This shape is probably the result of wet etching processing.

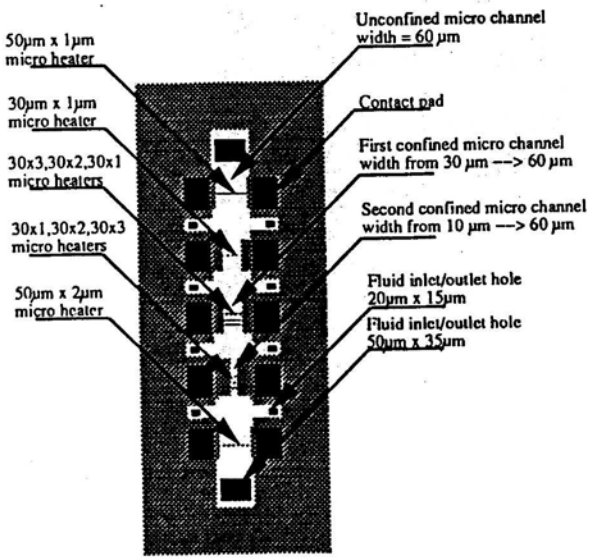

Figure 1 Schematic Layout of a Micro Channel.

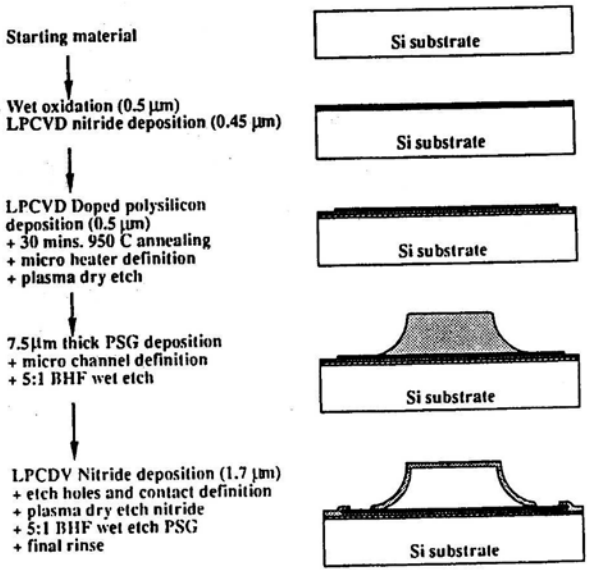

Figure 2 Process Steps in Fabricating Micro Heaters and Micro Channels.

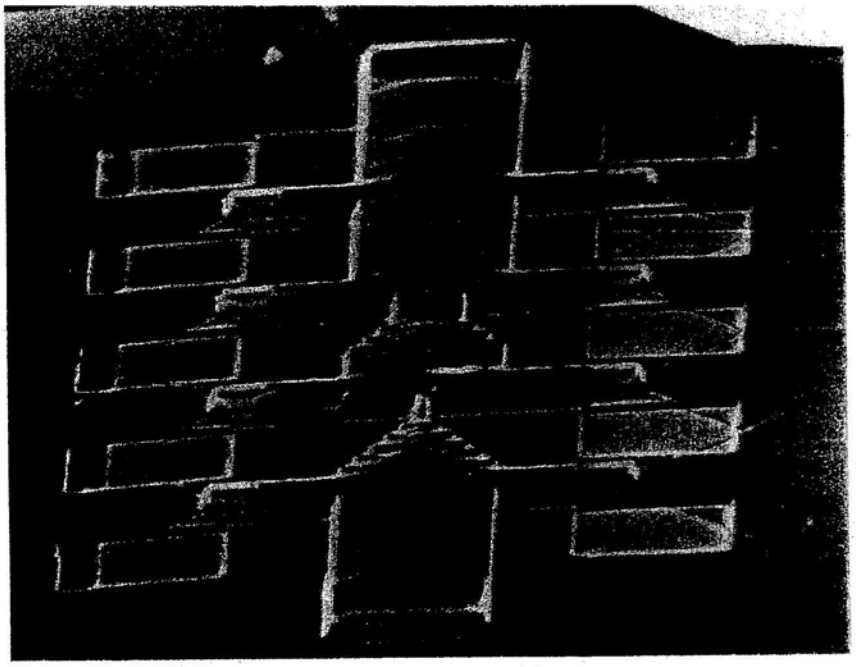

Figure 3 SEM Micrograph of a Fabricated Micro Channel.

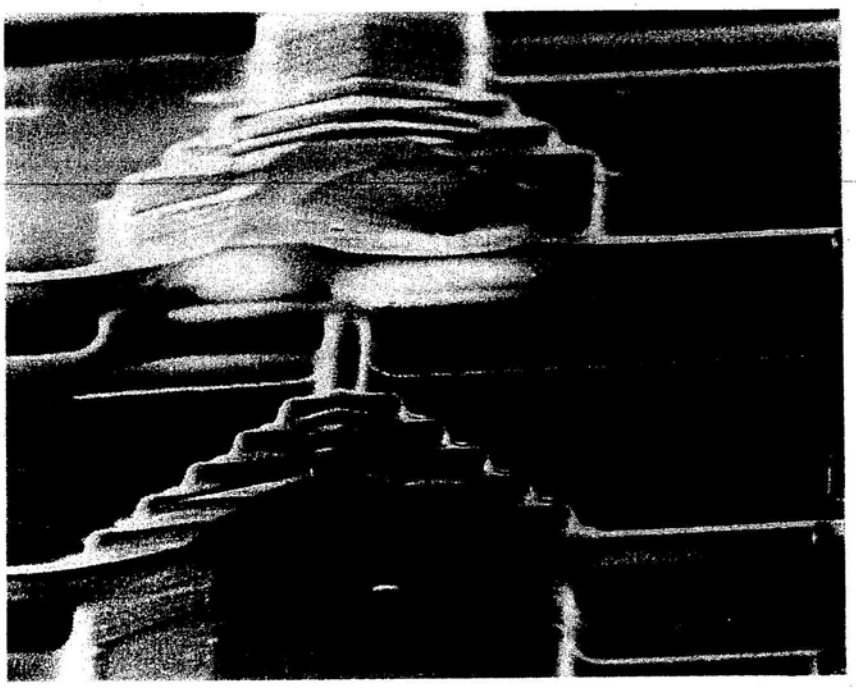

Figure 4 Closeup SEM View of the Confined Portion of the Micro Channel. For This Particular Sample, a Rare Fabrication Defect (Above the Center of the Picture) is Found.

The experimental setup is shown in Fig. 6. Current can be applied to the heater through the two contact pads. Two probe tips are positioned by micromanupilator in contact with the contact pads. An ammeter is connected in the circuit to measure the input current. The device is then immersed in a 5 mm deep pool of liquid and observed under a microscope. A Polaroid camera is attached to the microscope to document the bubble formation processes.

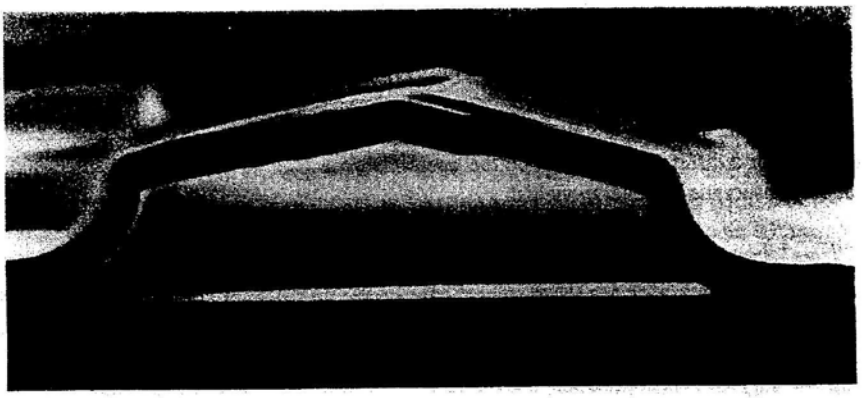

Figure 5 Cross Section SEM Micrograph of the Micro Channel. The Thickness of the Nitrate Cap is 1.7 μm and the Micro Channel is 30 μm in Width, 6 μm (edge) to 7.5 μm (Center) in Height.

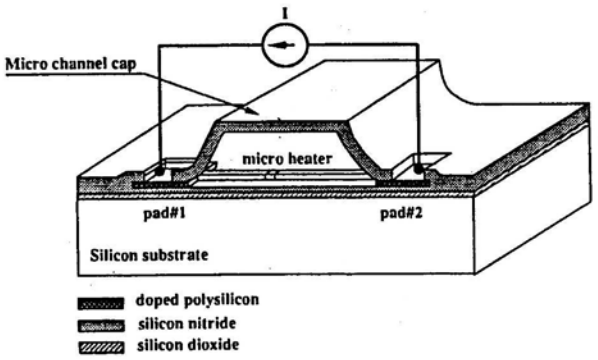

Figure 6 Experimental Setup for Bubble Formation on a Micro Heater Inside of the Micro Channel.

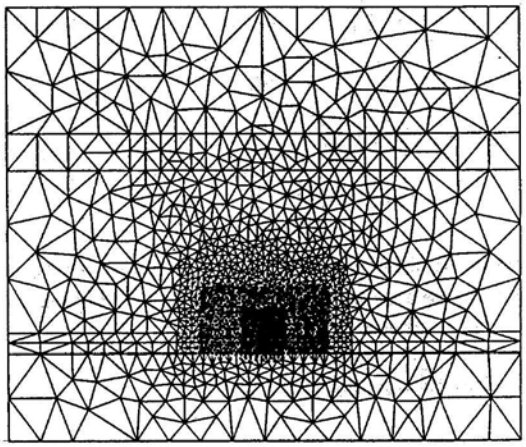

Figure 7 Finite Element Mesh for the Two-Dimensional Heat Conductiion Analysis. There are 2797 Triangular Elements.

3. Modeling of Micro Line Heaters

Bubble formation on the micro heaters within the microchannel is governed by the thermal field induced by the joule heating of the resistive heater elements. In reality, the thermal field is three-dimensional. However, the salient features of the steady-state heating process can be captured by neglecting the temperature variations in the direction perpendicular to the channel axis in plan view. Therefore, a two dimensional steady-state conduction analysis of the temperature field near the micro heater is performed to evaluate the thermal conduction excess flux shape factor [15]. This analysis also provides the temperature field information in the other two dimensions which are not included in the lumped one-dimensional, transient model developed in this paper.

This two-dimensional, steady-state analysis assumes negligible convection before the bubble is formed. A commercially available finite element solver [16] is used for solving the temperature field. The gridding for a 1 μm wide heater is shown in Fig. 7, representing 2797 triangular elements of decreasing size near the heater. Ten dimensionless steady state isotherms are illustrated in Fig. 8. The values of each isotherm shown represent differing values of $(T_{SS} - T_0)/10$. As implied in this figure, nearly all of the energy dissipated during the joule heating of the micro heater is conducted into the substrate rather

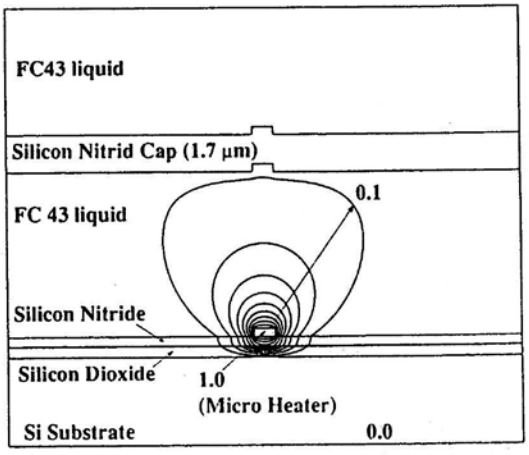

Figure 8 Isothermal Lines in a Plane Perpendicular to the Micro Heater Axis.

than conducted into the fluid. It is of note that the Rayleigh number, based on the channel height and the difference between the heater temperature and the ambient temperature, is of the order of 0.01. Therefore, the assumption of negligible fluid convection before bubble formation is justified.

The lumped, one dimensional model is developed from the law of energy conservation. For a differential element on the line heater shown in Fig. 6, the conservation of energy yields:

$$\frac{\partial U}{\partial t} = p_g + \dot{q}_{cond} + \dot{q}_{conv} + \dot{q}_{rad} \tag{1}$$

where $\frac{\partial U}{\partial t}$ is the rate of change in internal energy of the differential element, p_g is the electrical energy dissipated in the element and $\dot{q}_{cond}$, $\dot{q}_{conv}$ and $\dot{q}_{rad}$ are heat conduction, convection and radiation terms, respectively. Since the Rayleigh number for the micro line heaters has been calculated to be on the order of 0.01, the heat convection term, $\dot{q}_{conv}$ is neglected. The heat radiation term, $\dot{q}_{rad}$ has little contribution for the moderate temperatures and can be neglected [8]. The other terms can be represented as :

$$\frac{\partial U}{\partial t} = c_p \rho_p wz \Delta x \frac{\partial x}{\partial t} \tag{2}$$

$$p_g = J^2 r_o wz Dx [1 + \xi (T - T_o)] \tag{3}$$

$$\dot{q}_{cond} = k_p wz \left(\left[\frac{\partial T}{\partial x} \right]_x - \left[\frac{\partial T}{\partial x} \right]_{x+Dx} \right) + wDx k_{n+o} \frac{(T - T_o)}{(t_o + t_n)} \tag{4}$$

By substituting the above terms into Eqn. 1 and taking Δx as a differential operator, a second order partial differential heat equation can be derived as :

$$\frac{\partial^2 T}{\partial x^2} = \frac{1}{\alpha_p} \frac{\partial T}{\partial t} + \varepsilon (T - T_r) \tag{5}$$

where

$$\alpha_p = \frac{k_p}{c_p \rho_p} \tag{6}$$

$$\varepsilon = \frac{k_{n+o}}{k_p} \frac{1}{z(T_o + T_n)} - \frac{J^2 \rho_o \xi}{k_p} \tag{7}$$

and

$$T_r = \frac{k_{n+o}}{k_p} \frac{1}{z(t_o + t_n)} \frac{T_o}{\varepsilon} + \frac{J^2 \rho_o}{k_p} - \frac{J^2 \rho_o \xi}{k_p} \frac{T_o}{\varepsilon} \tag{8}$$

Where α_p is the thermal diffusivity of the polysilicon and both ε and T_r are functions of dimensions and the thermal properties of the micro heater and the thermal barriers. The k_{n+o} term used in Eqn. (4) is the combined thermal conductivity of the thermal barrier layer underneath the micro heater including the silicon nitride and the silicon dioxide layer and can be expressed as:

$$k_{n+o} = \frac{k_n k_o (t_n + t_o)}{k_o t_n + k_n t_o} F_s \tag{9}$$

The excess flux shape factor, F_S, is used to account for the additional heat conduction fluxes into the liquid and into the substrate at the corners of the heater. This excess flux shape factor is defined as the total heat flux out of the heater per unit length divided by the heat flux going directly under the heater only.

$$F_s = \frac{\textit{total heat flux per unit length}}{\frac{w k_{n+o}}{t_n + t_o}} \tag{10}$$

The excess flux shape factors are calculated and listed in Table I for different liquids (FC43, DI water, Methanol) and different heater widths (1 and 2 μm) used in this paper.

Eqn.(5) can be solved analytically by imposing initial ($T(x,t=0) = T_0$) and boundary ($T(x=0,t) = T_0$), ($T(x=L,t) = T_0$)) conditions. The steady state and transient solutions for the temperature along the heater are:

$$T(x)_{ss} = T_r - (T_r - T_o) \frac{\cosh\left(\sqrt{\varepsilon}\left(x - \frac{L}{2}\right)\right)}{\cosh\left(\sqrt{\varepsilon}\frac{L}{2}\right)} \tag{11}$$

$$T(x,t)_{tran} = e^{-\alpha_p \varepsilon t} \sum_{n=1}^{\infty} B_n \sin\left(\frac{n\pi x}{L}\right) e^{-\alpha_p t \left(\frac{n\pi}{L}\right)^2} \tag{12}$$

$$B_n = \frac{2}{L} \int_0^L (T_o - T(x)_{ss}) \sin\left(\frac{n\pi x}{L}\right) dx \tag{13}$$

By examining the transient solution, it is found that for the micro heaters used in this paper, the slowest transient decay time (n = 1) is at the order of 10 μ seconds. For an input source of frequency less than 10 kHz, the micro heater temperature will reach steady state. The maximum temperature is found to be at the center of the heater and can be expressed as :

$$T_{ssmax} = T_r - (T_r - T_o) \frac{1}{\cosh\left(\sqrt{\varepsilon}\frac{L}{2}\right)} \tag{14}$$

Table 1. Excess Flux Shape Factors for Micro Line Heaters in Different Liquids.

Width	FC 43	Water	Methanol
1 μm	2.25	2.67	2.38
2 μm	1.63	1.86	1.69

Thus, the maximum steady state heater temperature can be calculated directly from the thermal properties of the fluid and solids, and from the current density and electrical resistivity of the heater material.

The experiments were carried out by fixing the specimen in the bottom of a shallow beaker, pouring liquid into the beaker to about a 5 mm depth, passing current through the micro heater, and observing bubble nucleation. Both DC and AC sources were tested. It was observed that a minimum current is required for bubble formation under DC inputs. The micro bubble can be repeatedly formed under AC input below the frequency of about 100 Hz. For AC inputs above 100 Hz, the results are similar to those of DC input. These observations for bubble nucleation inside of micro channels are similar to the bubble formation in an open environment reported before [8].

Three different liquids have been tested, including Fluorinert FC43, deionized water and methanol. The bubble forming currents have been plotted with corresponding maximum

temperature calculated by Eqn. 14 as shown in Fig. 9. It is observed in Fig. 9 that the bubble nucleation temperatures are near the critical temperature of each liquids and these results are again the same as in previous work where the bubble formation processes have been observed in an open environment [8].

However, bubble formation in micro channels has several different features than bubble formation in an open environment. First, the micro bubble in straight micro channels have elliptical shapes rather than spherical shapes. This is shown in Figure 10, where an elliptical shape bubble is formed on the 50x1 μm^2 micro heater (the top heater in Fig. 1 and Fig. 3) immersed in FC 43 liquid. In this case,
the micro bubble has axial lengths of 60 and 16 μm and the

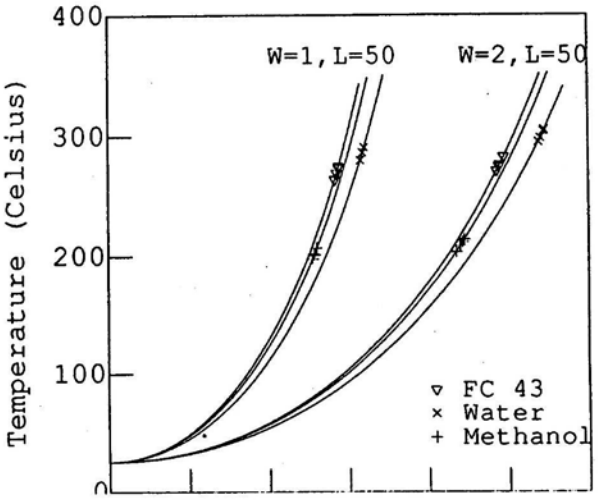

Figure 9. Measured Bubble Nucleation Currents and Calculated Temperatures for Two Widths of the Heater Inside the Micro Channel.

Figure 10 Micrograph of an Elliptical Bubble on a 50x1 μm^2 Line Heater on an Unconfined Substrate.

vertical dimension is assumed to be about 7.5 μm since it is confined above. Furthermore, the total bubble volumes are less than the spherical bubbles formed in open environment, where spherical bubbles of diameter nearly equal to the micro heater length were formed.

Other differences between the bubble formation processes were observed in the confined and unconfined channels. Fig. 11(a) shows the top confined portion of the micro channel shown in Fig. 1 immersed in FC43 liquid with two probe tips attached on both contact pads but without any input power. Fig. 11(b) shows the bubble at 30 mA of current, where the micro bubble fills the space near the heater in the confined micro channel and has a shape of about 30 μm at the top and 50 μm at the center portion. Fig. 11(c) shows the micro bubble at 35 mA of current at 8 minutes. The bubble is still growing but with a very slow speed such that a distinct, unblurred bubble image is observed in the photo even though the exposure period was 5 full seconds. Fig. 11(d) shows the situation after removing the input power. A circular shape bubble about 30 μm in diameter is ejected from the confined portion and advanced to the unconfined portions where the height and width are slightly larger. The bubble will condense back to liquid within tens of seconds depending on the initial size of the bubble and the heating condition. Fig. 11(e) shows the micro bubble in the micro channel under going the process of condensation and a black, huge micro bubble outside of the micro channel. This micro bubble on the right hand side of the photo has been formed on purpose by reducing the contact force of the right hand side probe, which results in a high contact resistance. Due to the electric energy dissipation across this contact resistance, a micro bubble of about 100 μm diameter has been formed for qualitative visual comparison of the bubble formation phenomenon inside and outside of micro channels. Fig. 11(f) is the micro bubble formation in a unconfined channel with exact same heater dimensions in Fig. 11(a) through (e). It is observed that micro bubbles formed in the unconfined channel are nondirectional, where a circular shape bubble of about 60 μm diameter is formed as compared with the bullet like shape of micro bubble in the confined micro channel as shown in Fig. 11(c).

Discussion and Conclusions

The mechanism for the micro bubble formation in the micro channels is of particular interest for applications of micro scale phase change, including bubble-jet printers. It is found previously that the bubble formation mechanism strongly depends on the maximum temperature on the micro heater [8] and this conclusion is again drawn for bubble formation inside the micro channel. The micro bubble apparently has a bursting nucleation mechanism at the temperature near the critical temperature where a visible bubble is formed abruptly. The FC 43 liquid and water have boiling temperatures of 174°C and 100°C respectively and critical temperature of 294°C and 374°C respectively. However, by examining Fig. 9, it is clear that a higher heater temperature is needed for bubble nucleation in water. These nucleation temperatures in Fig. 9 for each liquid are about 80% to 90% of their critical temperatures respectively, and this preliminary observation is consistent with homogeneous bubble nucleation temperature measurements reported before [17,18], even though

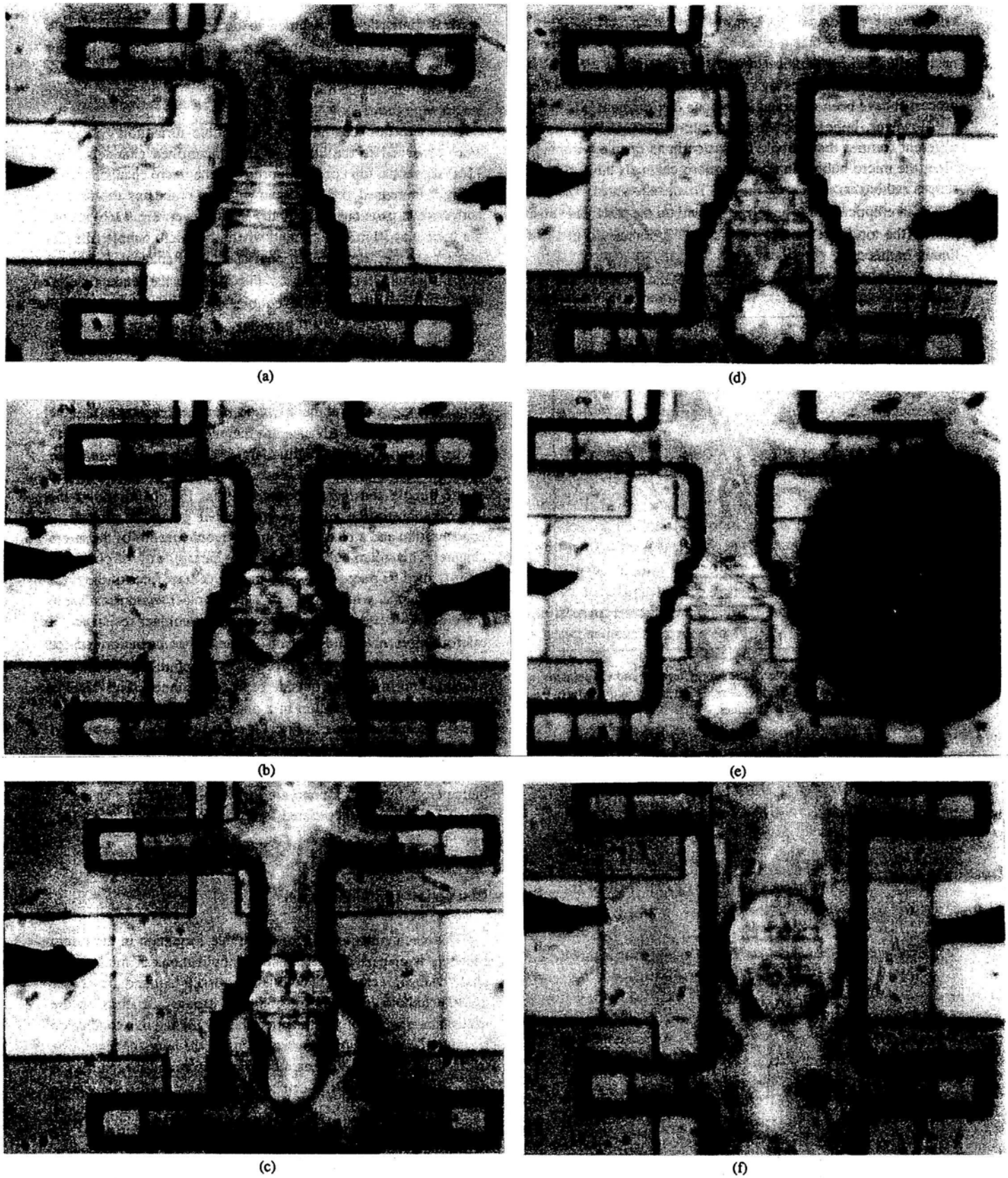

Figure 11. (a) Micrograph (Under an Optical Microscope) of a Confined Micro Channel With Width Diverging From 30 μm to 60 μm Under no Input Current. (b) Bubble Formation Under 30 mA of Input Current. The Two Black Objects are Probe Tips. (c) Bubble Formation Under 35 mA for 8 Mins. The Bubble has a Preferred Downward Movement With a Bullet-Like Shape. (d) After Removing the Input Power of (c), The Bubble Moves to a Preferred Position Where the Channel has the Maximum Height of 7.5 μm. (e) Two Micro Bubbles Shown in one Micrograph. The one Inside the Micro Channel is White and is in the Process of Condensation. The Other one Outside the Micro Channel is Black, Larger, and in the Process of Growing. (f) Micro Bubble Formation in an Unconfined Channel. The Bubble has no Preferred Direction of Movement.

this paper presents a very different experimental environment attribute to the dimension of the micro heaters. However, since the air solubility in FC 43 is much higher than that in water and the dissolved gas may also contributed to these preliminary results [19].The one-dimensional model presented in this paper is considered to be reasonably accurate in predicting the maximum heater surface temperature. The model predicts that the bubble forming temperatures are quite consistent for different liquids on different sizes of micro heaters. Theoretically, both the 50x1 and 30x1 μm^2 heaters should provide the same heater temperature under same current inputs since the length of the heater has little effect according to Eqn. 14. But a slightly less currents was measured on the 50x1 μm^2 heaters at the point of bubble nucleation and this may be caused by the trapezoidal shape of the micro channel and/or the deficiencies of the one-dimensional model.

Moreover, currents required for bubble formation are slightly different for the same heaters located on different silicon dies. Asai [20] has used a probability theory to explain similar phenomenon for heaters in Canon's bubble jet printer. It is likely that fabrication defects such as etching defects, corner effects and thickness variations are the major cause of these variations for micro line heaters presented in this paper. Nevertheless, these variations are relatively small and are not particular important for real applications.

The bubble formation in a confined, variable cross section micro channel can cause preferred bubble movement as shown in Fig. 11. The movement of the bubble to a larger cross section location is due to interfacial tension forces. The surface energy associated with an equal volume bubble is less in the larger dimension locations than in the confined region near the heater. It has also been observed that on the same portions of the micro channel, piston-like bubble movement can be produced by controlling the input current. The back and forth movement is due to the local Marangoni effect, where axial temperature gradients produce bubble-liquid interfacial shear, inducing fluid flow and thus bubble movement toward the heater during the heating cycle. Furthermore, the growing of a micro bubble in a micro channel is much more difficult than in an open environment. The possible reason is that the vapor bubble pressure inside the micro channel is much larger due to the smaller radius of curvature as predicted by Young-Laplace equation. Thus the bubble occupies a greater portion of the area near the heater.

In conclusion, the bubble formation and movement processes in constant and variable cross-section transparent micro channels are complex and difficult to quantify. Much more experimental and theoretical work is required to fully describe the observations reported in this preliminary study. However, the dominant features of bubble formation and movement are relatively discernible.

Acknowledgments

The authors would like to thank Prof. V. P. Carey for valuable discussions, and 3M company for providing the FC liquids and Dr. A. P. Lee for assisting fabrication. These devices were fabricated in the U.C. Berkeley Microfabrication Laboratory. This work has been supported by the Berkeley Sensor and Actuator Center, an NSF/Industry/University Cooperative Research Center.

References

[1] D. B. Tuckerman and R. F. W. Pease, "High-Performance Heat Sinking for VLSI", *IEEE Electron Device Letters*, VOL. EDL-2, No. 5, pp. 126-129, May, 1981.

[2] T. L. Hoopman, "Microchanneled Structures", *Proceedings of ASME Winter Annual Meeting, Micromechanical Sensors, Actuators and Systems*, pp. 171-174, Dallas, Nov. 25-30, 1990.

[3] J. Pfahler, J. Harley, H. Bau and J. Zemel, "Liquid Transport in Micron and Submicron Channels", *Sensors and Actuators A-Physical*, Vol. 22, N1-3, pp. 431-434, March, 1990.

[4] J. Pfahler, J. Harley, H. Bau and J. Zemel , "Liquid and Gas Transport in Small Channels", *Proceedings of ASME Winter Annual Meeting, Micromechanical Sensors, Actuators and Systems*, pp. 149-158, Dallas, Nov. 25-30, 1990.

[5] A. Weisberg, H. Bau and J. Zemel , "Micro Heat Exchangers", Proceedings of ASME Winter Annual Meeting, *Micromechanical Sensors, Actuators and Systems*, pp. 159-170, Dallas, Nov. 25-30, 1990.

[6] R. W. Keyes, "Heat Transfer in Forced Convection Through Fins", *IEEE Trans. on Electron Device*, VOL. ED-31, No. 9, pp. 1218-1221, Sept., 1984.

[7] J. P. Longtin, B. Badran, and F. M. Gerner , "A One-Dimensional Model of a Micro Heat Pipe During Steady-State Operation", *Heat Transfer on the Microscale*, ASME HTD-Vol. 200, pp. 23-34, 1992.

[8] L. Lin and A. P. Pisano , "Bubble Forming on a Micro Line Heater", Proceedings of ASME Winter Annual Meeting, *Micromechanical Sensors, Actuators and Systems*, DSC-Vol. 32, pp. 147-163, 1991.

[9] L. Lin, A. P. Pisano and A. P. Lee, "Microbubble Powered Microactuator", *Digest of Transducers '91*, pp. 1041-1044, June 23-27, 1991.

[10] C. H. Mastrangelo, J. H. Yeh and R. S. Muller, "Electrical and Optical Characteristics of Vacuum-Sealed Polysilicon Microlamps", *IEEE Transactions on Electron Devices*, Vol. 39, pp. 1363-1375, June, 1992.

[11] L. A. Field, R. M. White and A. P. Pisano, "Fluid-Powered Rotary Gears and Micro-Flow Channels", *Digest of Transducers '91*, pp. 1033-1036, June 23-27, 1991.

[12] R. R. Allen, J. D. Meyer, and W. R. Knight, "Thermodynamics and Hydrodynamics of Thermal Ink Jets", *HP Journal*, pp. 21-27, May 1985.

[13] A. Asai, "Bubble Dynamics in boiling under High Heat Flux Pulse Heating", *ASME/JSME Thermal Engineering Proceedings*, Vol.. 2, pp. 269-274, 1991.

[14] S.-D. Oh, S.-S. Seung and H.-Y. Kwak, "A Model of Bubble Nucleation on a Micro Line Heater", Proceedings of ASME Winter Annual Meeting, *Micromechanical Sensors, Actuators and Systems*, Nov. 1992.

[15] J. P. Holman, "Heat Transfer", 7th ed. New York, McGraw-Hill Book Co., 1990.

[16] Maxwell Solver, v.4.33, Ansoft Corp., 4 Station Square, 660 Commerce Court Building, Pittsburgh, Pa. 15219.

[17] M. Blander and J. L. Katz, "Bubble Nucleation in Liquids", *AIChE Journal*, Vol. 21, pp. 833-847, September 1975.

[18] M. Blander, D. Hengstenberg, and J. L. Katz,, "Bubble Nucleation in n-Pentane, n-Hexane, n-Petane + Hexadecane Mixtures and Water", *Journal of Physical Chemistry*, Vol. 75, pp. 3613-3619, 1971.

[19] C. A. Ward, A. Balakrishnan, and F. C. Hooper, "On the Thermodynamics of Nucleation in Weak Gas-liquid Solutions", *J. Basic Eng.*, pp. 695-704, 1970.

[20] A. Asai, "Application of the Nucleation Theory to the Design of Bubble Jet Printers", *Japanese Journal of Applied Physics*, Vol. 28, pp. 909-915, May, 1989.